

1                   **High-order cognition is supported by complex but**  
2                   **compressible brain activity patterns**

3                   Lucy L. W. Owen<sup>1,2</sup> and Jeremy R. Manning<sup>1,\*</sup>

4                   <sup>1</sup>Department of Psychological and Brain Sciences,  
5                   Dartmouth College, Hanover, NH

6                   <sup>2</sup>Carney Institute for Brain Sciences,  
7                   Brown University, Providence, RI

8                   \*Address correspondence to jeremy.r.manning@dartmouth.edu

9                   February 27, 2023

10                  **Abstract**

11                  We applied dimensionality reduction algorithms and pattern classifiers to functional neuroimaging  
12                  data collected as participants listened to a story, temporally scrambled versions of the story, or underwent  
13                  a resting state scanning session. These experimental conditions were intended to require different depths  
14                  of processing and inspire different levels of cognitive engagement. We considered two primary aspects of  
15                  the data. First, we treated the number of features (components) required to achieve a threshold decoding  
16                  accuracy as a proxy for the “compressibility” of the neural patterns (where fewer components indicate  
17                  greater compression). Second, we treated the maximum achievable decoding accuracy across participants  
18                  as an indicator of the “stability” of the recorded patterns. Overall, we found that neural patterns recorded  
19                  as participants listened to the intact story required fewer features to achieve comparable classification  
20                  accuracy to the other experimental conditions. However, the peak decoding accuracy (achievable with  
21                  more features) was also highest during intact story listening. Taken together, our work suggests that  
22                  our brain networks flexibly reconfigure according to ongoing task demands, and that the activity patterns  
23                  associated with higher-order cognition and high engagement are both more complex and more compressible  
24                  than the activity patterns associated with lower-order tasks and lower levels of engagement.

25                  **Introduction**

26                  Large-scale networks, including the human brain, may be conceptualized as occupying one or more positions  
27                  along on a continuum. At one extreme, every node is fully independent of every other node. At the other  
28                  extreme, all nodes behave identically. Each extreme optimizes key properties of how the network functions.  
29                  When every node is independent, the network is maximally *expressive*: if we define the network’s “state”  
30                  as the activity pattern across its nodes, then every state is equally reachable by a network with fully  
31                  independent nodes. On the other hand, a network of identically behaved nodes optimizes *robustness*: any  
32                  subset of nodes may be removed from the network without any loss of function or expressive power, as  
33                  long as any single node remains. Presumably, most natural systems tend to occupy positions between  
34                  these extremes. We wondered: might the human brain reconfigure itself to be more flexible or more robust

30 according to ongoing demands? In other words, might the brain reconfigure its connections or behaviors  
31 under different circumstances to change its position along this continuum?

32 Closely related to the above notions of expressiveness versus robustness are measures of how much  
33 *information* is contained in a given signal or pattern, and how *redundant* a signal is (Shannon, 1948). Formally,  
34 information is defined as the amount of uncertainty about a given variables' outcomes (i.e., entropy),  
35 measured in *bits*, or the optimal number of yes/no questions needed to reduce uncertainty about the  
36 variable's outcomes to zero. Highly complex systems with many degrees of freedom (i.e., high flexibility  
37 and expressiveness), are more information-rich than simpler or more constrained systems. The redundancy  
38 of a signal denotes the difference how expressive the signal *could* be (i.e., proportional to the number of  
39 unique states or symbols used to transmit the signal) and the actual information rate (i.e., the entropy of  
40 each individual state or symbol). If a brain network's nodes are fully independent, then the number of bits  
41 required to express a single activity pattern is proportional to the number of nodes. The network would  
42 also be minimally redundant, since the status of every node would be needed to fully express a single brain  
43 activity pattern. If a brain network's nodes are fully coupled and identical, then the number of bits required  
44 to express a single activity pattern is proportional to the number of unique states or values any individual  
45 node can take on. Such a network would be highly redundant, since knowing any individual node's state  
46 would be sufficient to recover the full-brain activity pattern. Highly redundant systems are also robust,  
47 since there is little information loss from losing any given observation.

48 We take as a given that brain activity is highly flexible: our brains can exhibit nearly infinite activity  
49 patterns. This flexibility implies that our brains activity patterns are highly information rich. However,  
50 brain activity patterns are also highly structured. For example, full-brain correlation matrices are stable  
51 within (Finn et al., 2015, 2017; Gratton et al., 2018) and across (Yeo et al., 2011; Glerean et al., 2012; Gratton  
52 et al., 2018; Cole et al., 2014) individuals. This stability suggests that our brains' activity patterns are at  
53 least partially constrained, for example by anatomical, external, or internal factors. Constraints on brain  
54 activity that limit its flexibility decrease expressiveness (i.e., its information rate). However, constraints on  
55 brain activity also increase its robustness to noise (e.g., “missing” or corrupted signals may be partially  
56 recovered). For example, recent work has shown that full-brain activity patterns may be reliably recovered  
57 from only a relatively small number of implanted electrodes (Owen et al., 2020; Scangos et al., 2021). This  
58 robustness property suggests that the relevant signal (e.g., underlying factors that have some influence over  
59 brain activity patterns) are compressible.

60 To the extent that brain activity patterns contain rich task-relevant information, we should be able to  
61 use the activity patterns to accurately differentiate between different aspects of the task (e.g., using pattern  
62 classifiers; Norman et al., 2006). For example, prior work has shown a direct correspondence between

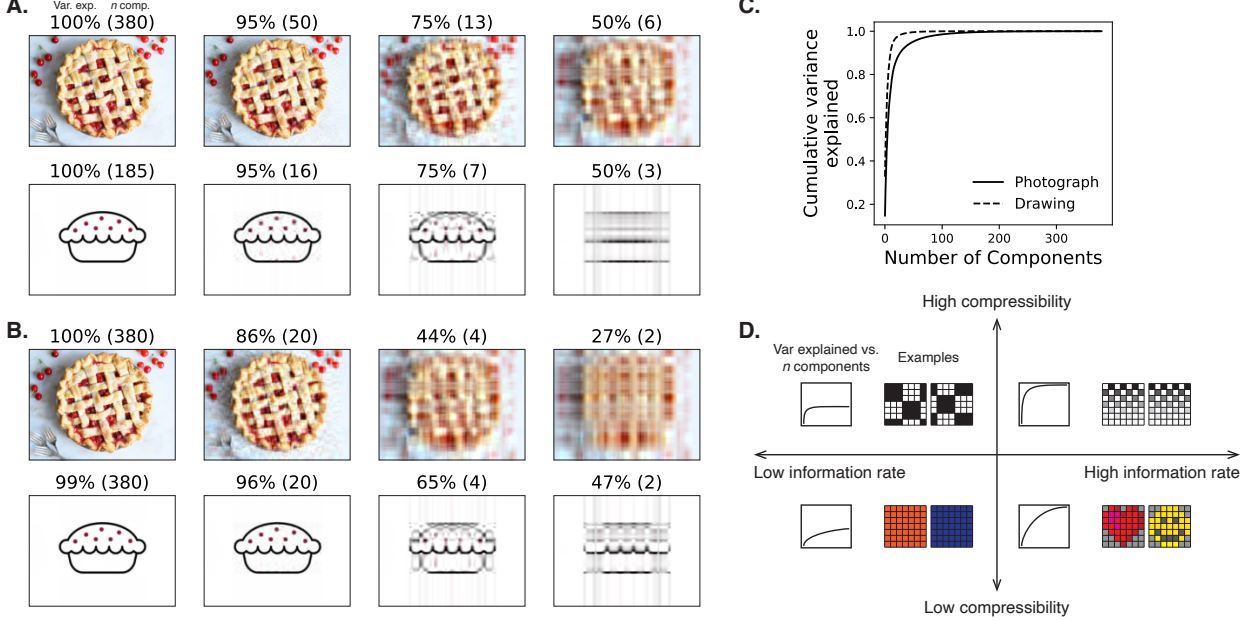


**Figure 1: Information content and compressibility.** **A. Variance explained for two images.** We applied principal components analysis to a photograph and drawing, treating each row of the images as “observations.” Across columns, we identified the number of components required to explain 100%, 95%, 75%, or 50% of the cumulative variance in each image (the 100% columns denote the original images). The numbers of components are indicated in parentheses, and the resulting “compressed” images are displayed. **B. Representing two images with different numbers of components.** Using the same principal component decompositions as in Panel A, we computed the cumulative proportion of variance explained with 380 (original images), 20, 4, or 2 components. **C. Cumulative variance explained versus number of components.** For the images displayed in Panels A and B, we plot the cumulative proportion of variance explained as a function of the number of components used to represent each image. **D. Information rate and compressibility.** Across multiple images, the information rate (i.e., the amount of information contained in each image; horizontal axis) is high when each individual pixel provides information that cannot be inferred from other pixels. High-information rate images tend to be high-resolution, and low-information rate images tend to be low-resolution. Compressibility is related to the difference between the information required to specify the original versus compressed images (vertical axis). Highly compressible images often contain predictable structure (redundancies) that can be leveraged to represent the images much more efficiently than in their original feature spaces.

63 classification accuracy and the information content of a signal (Alvarez, 2002). To the extent that brain  
64 activity patterns are compressible, we should be able to generate simplified (e.g., lower dimensional)  
65 representations of the data while still preserving the relevant or important aspects of the original signal.  
66 In general, information content and compressibility are related but are partially dissociable (Fig. 1). If a  
67 given signal (e.g., a representation of brain activity patterns) contains more information about ongoing  
68 cognitive processes, then the peak decoding accuracy should be high. And if the signal is compressible, a  
69 low-dimensional embedding of the signal will be similarly informative to the original signal (Fig. 1D).

70 Several recent studies suggest that the complexity of brain activity is task-dependent, whereby simpler  
71 tasks with lower cognitive demands are reflected by simpler and more compressible brain activity patterns,  
72 and more complex tasks with higher cognitive demands are reflected by more complex and less compressible  
73 brain activity patterns (Mack et al., 2020; Owen et al., 2021). These findings complement other work  
74 suggesting that functional connectivity (correlation) patterns are task-dependent (Finn et al., 2017; Owen  
75 et al., 2020; Cole et al., 2014), although see Gratton et al. (2018). Higher-order cognitive processing of a  
76 common stimulus also appears to drive more stereotyped task-related activity and functional connectivity  
77 across individuals (Hasson et al., 2008; Lerner et al., 2011; Simony & Chang, 2020; Simony et al., 2016).

78 The above prior studies are consistent with two potential descriptions of how cognitive processes are  
79 reflected in brain activity patterns. One possibility is that the information rate of brain activity increases during  
80 more complex or higher-level cognitive processing. If so, then the ability to reliably decode cognitive states  
81 from brain activity patterns should improve with task complexity or with the level (or “depth”) of cognitive  
82 processing. A second possibility is that the compressibility of brain activity patterns increases during  
83 more complex or higher-level cognitive processing. If so, then individual features of brain recordings, or  
84 compressed representations of brain recordings, should carry more information during complex or high-  
85 level (versus simple or low-level) cognitive tasks.

86 We used a previously collected neuroimaging dataset to estimate the extent to which each of these two  
87 possibilities might hold. The dataset we examined comprised functional magnetic resonance imaging (fMRI)  
88 data collected as participants listened to an audio recording of a 10-minute story, temporally scrambled  
89 recordings of the story, or underwent a resting state scan (Simony et al., 2016). Each of these experimental  
90 conditions evokes different depths of cognitive processing (Simony et al., 2016; Lerner et al., 2011; Hasson et  
91 al., 2008; Owen et al., 2021). We used across-participant classifiers to decode listening times in each condition,  
92 as a proxy for how “informative” the task-specific activity patterns were (Simony & Chang, 2020). We also  
93 use principle components analysis to generate lower-dimensional representations of the activity patterns.  
94 We then repeated the classification analyses after preserving different numbers of components and examined  
95 how classification accuracy changed across the different experimental conditions.

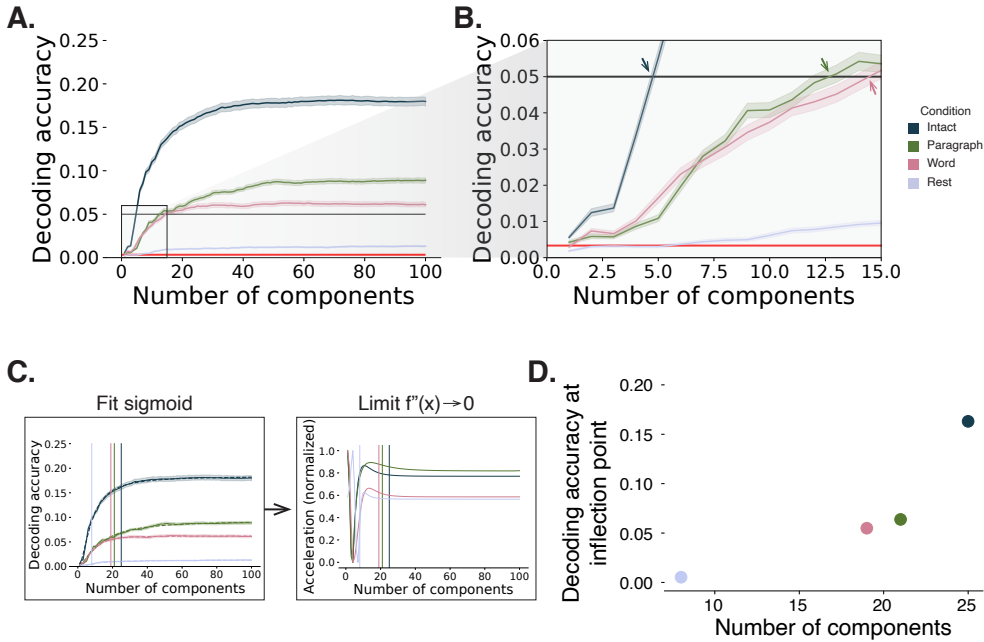


**Figure 2: Decoding accuracy and compression.** **A. Decoding accuracy by number of components.** Ribbons of each color display cross-validated decoding performance for each condition (intact, paragraph, word, and rest), as a function of the number of components (features) used to represent the data. The horizontal red line denotes chance performance, and the horizontal black line denotes 5% decoding accuracy (used as a reference in Panel B). **B. Numbers of components required to reach a fixed decoding accuracy threshold, by condition.** The panel displays a zoomed-in view of the inset in Panel A. Intersections between each condition's decoding accuracy curve and the 5% decoding accuracy reference line are marked by arrows. **C. Estimating inflection points.** We sought to identify an “inflection point” for each decoding curve, denoting the number of components at which the decoding curve asymptotes. We fit sigmoid functions to each decoding curve (left sub-panel) and then computed the minimum number of components where the second derivative of the sigmoid was both positive and less than a threshold value of 0.0001. **D. Inflection points by condition.** Each dot displays the number of components (x-axis) and decoding accuracy (y-axis) at one condition's inflection point. All error ribbons denote bootstrap-estimated 95% confidence intervals.

## 96 Results

## 97 Discussion

## 98 Methods

## 99 Acknowledgements

100 We acknowledge discussions with Rick Betzel, Emily Finn, and Jim Haxby. Our work was supported in part  
 101 by NSF CAREER Award Number 2145172 to J.R.M. The content is solely the responsibility of the authors  
 102 and does not necessarily represent the official views of our supporting organizations. The funders had no

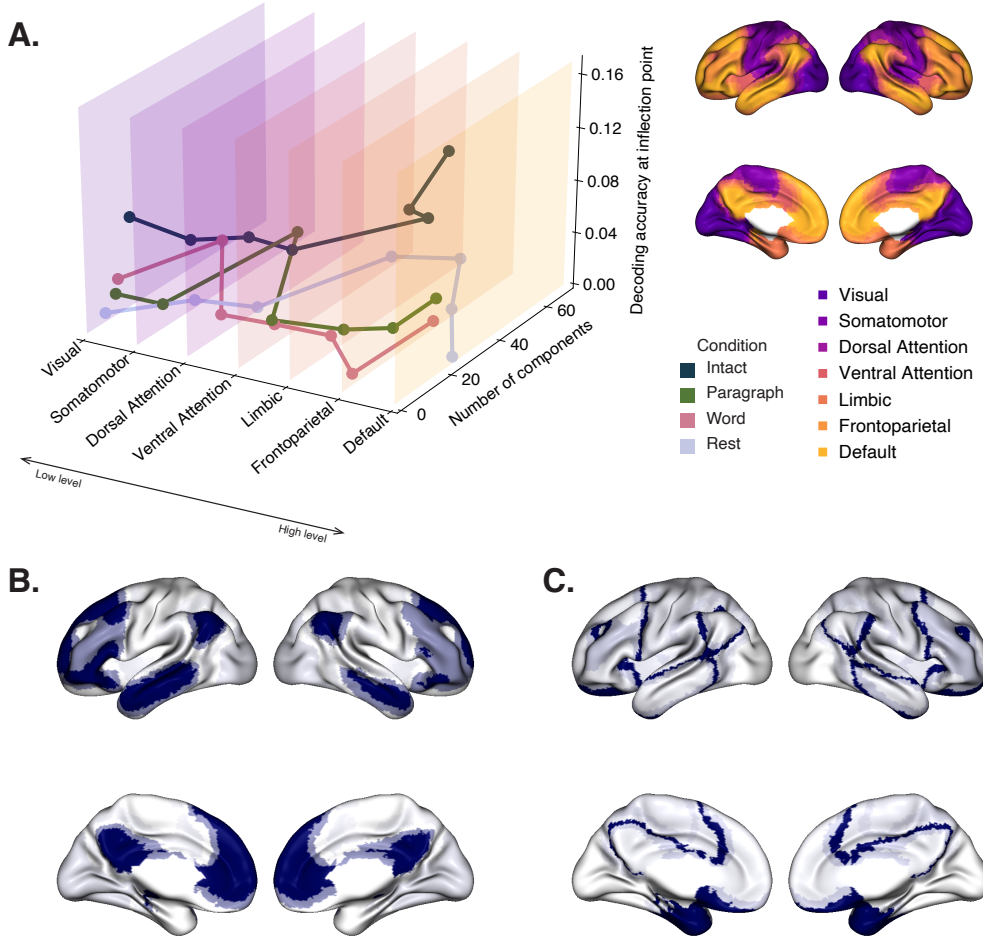


**Figure 3: Network-specific decoding accuracy and compression.** **A. Decoding accuracy and number of components for network-specific inflection points.** We considered the seven networks identified by Yeo et al. (2011). We computed each network's inflection point, for each experimental condition, using the procedure described in Figure 2C. **B. Network-specific decoding accuracy.** Each of the seven networks are colored according to the decoding accuracy at the network's inflection point for the "intact" experimental condition (corresponding to the dark blue curve in Panel A). **C. Network-specific compression.** Each of the seven networks are colored according to the number of components at the network's inflection point for the intact experimental condition. Larger numbers of components reflect lower compressibility.

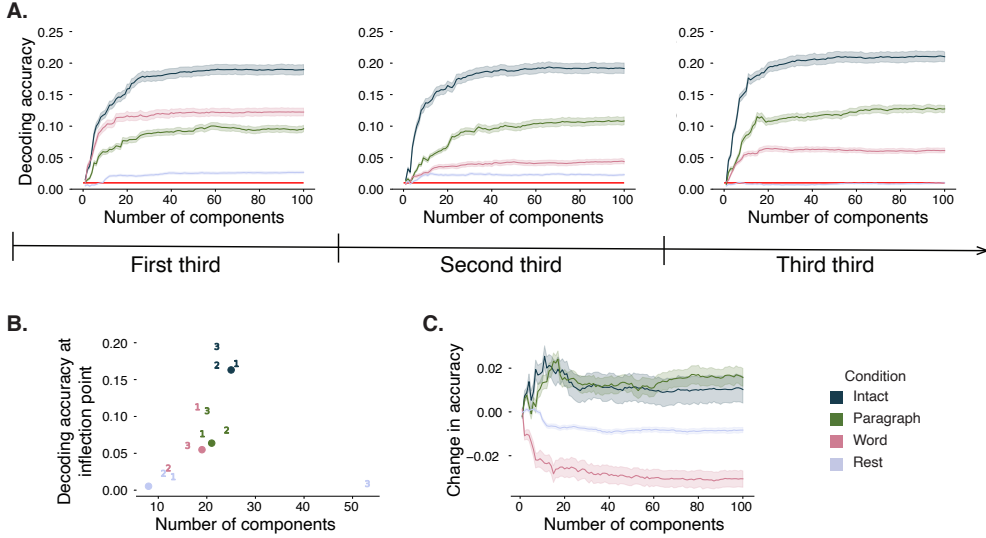


**Figure 4: Changes in decoding accuracy and compression over time. A. Decoding accuracy by number of components, by story segment.** Each family of curves is plotted in the same format as Figure 2A but reflects data only from one third of the dataset. **B. Inflection points by condition and segment.** The dots re-plot the inflection points from Figure 2D for reference. The numbers denote the inflection points for each third of the dataset (1: first third; 2: second third; 3: third third; colors denote experimental conditions). **C. Change in decoding accuracy over time, by number of components.** For each number of components (*x*-axis) and condition (color), we fit a regression line to the decoding accuracies obtained for the first, second, and third thirds of the dataset (corresponding to the left, middle, and right columns of Panel A, respectively). The *y*-axis denotes the slopes of the regression lines. All error ribbons denote bootstrap-estimated 95% confidence intervals.

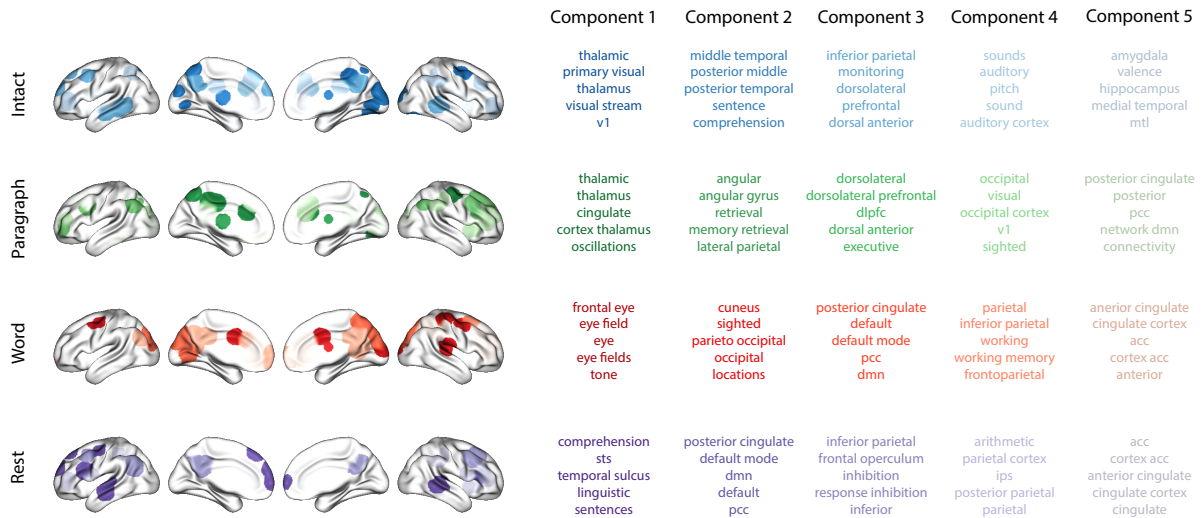


**Figure 5: Top terms associated with the highest-weighted components by condition.** Each row corresponds to an experimental condition, and the colors correspond to the component number (ranked by proportion of variance explained). The inflated brain plots display the spatial distributions of each components' hubs (see *Topographic Factor Analysis*). The lists on the right display the top five Neurosynth terms (Rubin et al., 2017) decoded from each components' brain map. Analogous maps computed separately for each story segment may be found in Figure S1.

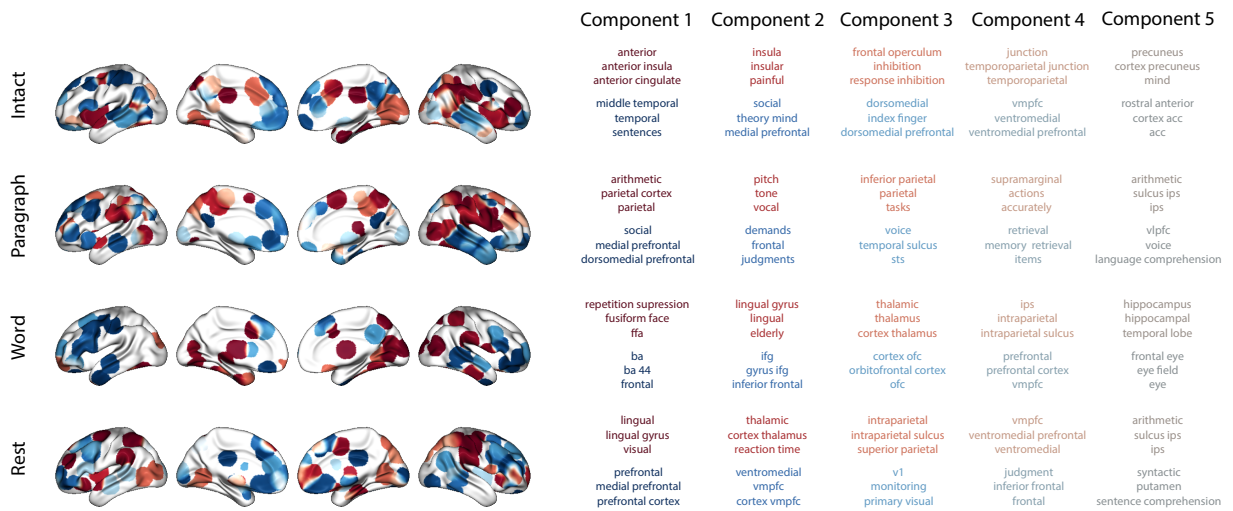


**Figure 6: Changes in decoding accuracy and compression over time.** Each row corresponds to an experimental condition, and the colors correspond to change direction (positive: red; negative: blue). The saturation denotes the component number (columns on the right). The lists on the right display the top five Neurosynth terms (Rubin et al., 2017) decoded from each components' brain map.

103 role in study design, data collection and analysis, decision to publish, or preparation of the manuscript.

## 104 Author contributions

105 Conceptualization: J.R.M. and L.L.W.O. Methodology: J.R.M. and L.L.W.O. Implementation: L.L.W.O. Analysis: L.L.W.O. Writing, Reviewing, and Editing: J.R.M. and L.L.W.O. Supervision: J.R.M.

## 107 References

- 108 Alvarez, S. A. (2002). *An exact analytical relation among recall, precision, and classification accuracy in information retrieval* (Technical Report No. BCCS-02-01). Boston College.
- 109 Cole, M. W., Bassett, D. S., Power, J. D., Braver, T. S., & Petersen, S. E. (2014). Intrinsic and task-evoked network architectures of the human brain. *Neuron*, 83(1), 238–251.
- 110 Finn, E. S., Scheinost, D., Finn, D. M., Shen, X., Papademetris, X., & Constable, R. T. (2017). Can brain state be manipulated to emphasize individual differences in functional connectivity. *NeuroImage*, 160, 140–151.
- 111 Finn, E. S., Shen, X., Scheinost, D., Rosenberg, M. D., Huang, J., Chun, M. M., ... Constable, R. T. (2015). Functional connectome fingerprinting: identifying individuals using patterns of brain connectivity. *Nature Neuroscience*, 18, 1664–1671.

- 117 Glerean, E., Salmi, J., Lahnakoski, J. M., Jääskeläinen, I. P., & Sams, M. (2012). Functional magnetic resonance  
118 imaging phase synchronization as a measure of dynamic functional connectivity. *Brain Connectivity*, 2(2),  
119 91–101.
- 120 Gratton, C., Laumann, T. O., Nielsen, A. N., Greene, D. J., Gordon, E. M., Gilmore, A. W., ... Petersen, S. E.  
121 (2018). Functional brain networks are dominated by stable group and individual factors, not cognitive or  
122 daily variation. *Neuron*, 98(2), 439–452.
- 123 Hasson, U., Yang, E., Vallines, I., Heeger, D. J., & Rubin, N. (2008). A hierarchy of temporal receptive  
124 windows in human cortex. *The Journal of Neuroscience*, 28(10), 2539–2550.
- 125 Lerner, Y., Honey, C. J., Silbert, L. J., & Hasson, U. (2011). Topographic mapping of a hierarchy of temporal  
126 receptive windows using a narrated story. *The Journal of Neuroscience*, 31(8), 2906–2915.
- 127 Mack, M. L., Preston, A. R., & Love, B. C. (2020). Ventromedial prefrontal cortex compression during  
128 concept learning. *Nature Communications*, 11(46), doi.org/10.1038/s41467-019-13930-8.
- 129 Norman, K. A., Polyn, S. M., Detre, G. J., & Haxby, J. V. (2006). Beyond mind-reading: multi-voxel pattern  
130 analysis of fMRI data. *Trends in Cognitive Sciences*, 10(9), 424–430.
- 131 Owen, L. L. W., Chang, T. H., & Manning, J. R. (2021). High-level cognition during story listening is  
132 reflected in high-order dynamic correlations in neural activity patterns. *Nature Communications*, 12(5728),  
133 doi.org/10.1038/s41467-021-25876-x.
- 134 Owen, L. L. W., Muntianu, T. A., Heusser, A. C., Daly, P., Scangos, K. W., & Manning, J. R. (2020). A Gaussian  
135 process model of human electrocorticographic data. *Cerebral Cortex*, 30(10), 5333–5345.
- 136 Rubin, T. N., Kyoejo, O., Gorgolewski, K. J., Jones, M. N., Poldrack, R. A., & Yarkoni, T. (2017). Decoding  
137 brain activity using a large-scale probabilistic functional-anatomical atlas of human cognition. *PLoS  
138 Computational Biology*, 13(10), e1005649.
- 139 Scangos, K. W., Khambhati, A. N., Daly, P. M., Owen, L. L. W., Manning, J. R., Ambrose, J. B., ... Chang,  
140 E. F. (2021). Biomarkers of depression symptoms defined by direct intracranial neurophysiology. *Frontiers  
141 in Human Neuroscience*, In press.
- 142 Shannon, C. E. (1948). A mathematical theory of communication. *Bell System Technical Journal*, 27(3),  
143 379–423.
- 144 Simony, E., & Chang, C. (2020). Analysis of stimulus-induced brain dynamics during naturalistic paradigms.  
145 *NeuroImage*, 216, 116461.

- <sup>146</sup> Simony, E., Honey, C. J., Chen, J., & Hasson, U. (2016). Dynamic reconfiguration of the default mode  
<sup>147</sup> network during narrative comprehension. *Nature Communications*, 7(12141), 1–13.
- <sup>148</sup> Yeo, B. T. T., Krienen, F. M., Sepulcre, J., Sabuncu, M. R., Lashkari, D., Hollinshead, M., . . . Buckner, R. L.  
<sup>149</sup> (2011). The organization of the human cerebral cortex estimated by intrinsic functional connectivity.  
<sup>150</sup> *Journal of Neurophysiology*, 106(3), 1125–1165.